

Recent Trends in the Spatial Structure of Wind Forcing and SST in the California Current System

FRANKLIN SCHWING

RICHARD PARRISH

ROY MENDELSSOHN

Pacific Fisheries Environmental Group
(PFEG)
1352 Lighthouse Avenue
Pacific Grove
CA 93950-2097
USA

ABSTRACT

State-space statistical models are applied to long time series of monthly COADS northward wind stress and sea surface temperature (SST) from the California Current System (CCS) for the period 1946-1990. The models estimate a non-parametric and non-linear trend, a non-stationary and non-deterministic seasonal signal, and an autoregressive (AR) term. They are also applied to long SST time series from selected coastal sites for comparison to the COADS series. SST shows decadal-scale periods of warm and cool anomalies that extend through the entire CCS. Wind stress anomalies are less extensive latitudinally and generally uncorrelated with SST, suggesting that decadal-scale SST variations in the CCS are controlled by fluctuations in the basin- to global-scale pressure and wind fields, rather than local wind forcing.

The CCS can be divided into three distinct geographical regions, which are similar to the system's biological regions. The northern region of the CCS (42-48°N) features a transition from strongly equatorward to poleward stress with distance north. The mean stress north of 44°N is poleward and has become increasingly poleward over time. This region features spatially uniform SST that has cooled over time. Winds south of 42°N are equatorward and can be described in terms of a central and southern region. The central region (34-42°N) exhibits the

strongest wind stress in the CCS; equatorward stress has increased over time more than in the northern and southern regions. This region features the greatest interannual to decadal variation in stress and SST as well. Stress in the southern region (22-34°N) has become increasingly equatorward over time in a relatively monotonic pattern. Mean SST decreases consistently with increasing latitude in the central and southern regions. SST off California warms rapidly in response to ENSO events as well as the 1976 regime shift, but much more slowly at other latitudes. While SST along the entire coast has warmed during the past several decades, offshore SST has cooled north of 36°N. This long-term cooling in the northern CCS is linked to large-scale cool anomalies in the central north Pacific rather than changes in local wind forcing. A different complex of processes is responsible for the long-term coastal warming tendency. It also appears that distinct combinations of wind-forced advection, mixing and direct heating lead to significantly different regional responses of the coastal ocean to climate change, which in turn may have substantial consequences for marine populations in eastern boundary current ecosystems.

RÉSUMÉ

Des séries mensuelles de la tension méridienne du vent et de la température de surface du système du courant de Californie, issues de la base de données COADS sur la période 1946-1990, sont décomposées à l'aide de modèles Espace-Etat. Ces modèles estiment de façon non paramétrique une tendance non linéaire, un signal saisonnier non déterministe et non stationnaire, et un terme autorégressif. Pour pouvoir effectuer des comparaisons, des séries de températures de surface provenant de quelques sites côtiers ont également été décomposées par les mêmes méthodes statistiques. On montre qu'il existe pour la température de surface de la mer, des périodes d'anomalies chaudes ou froides à l'échelle décennale sur l'ensemble du système du courant californien. Les anomalies de la tension du vent s'étendent moins en latitude et sont généralement non corrélées avec les anomalies observées dans les températures de surface. Ceci suggère que les variations décennales de température de surface sont contrôlées par des champs de pression et de vent à une échelle globale plutôt que par le forçage local du vent. Le système du courant de Californie peut être divisé en trois régions correspondant à trois écosystèmes différents. La région nord (42-48 °N) est une zone de transition entre des vents dirigés vers l'équateur au sud de cette zone et vers le pôle au nord de 44 °N. Cette orientation vers le

pôle a tendance à s'accroître avec le temps. De même, la température de surface de la mer, relativement homogène dans la région (42°-48 °N), a tendance à diminuer. Au sud de 42 °N, la direction du vent est orientée vers l'équateur, cette latitude détermine la séparation entre la région nord et les régions centrale et sud. C'est dans la région centrale (34°-42 °N) que la tension du vent est la plus forte et que l'augmentation de la composante sud du vent a été la plus importante. C'est aussi dans la région centrale que les variations interannuelles et décennales de la tension de vent et de la température de surface sont les plus grandes. La composante sud du vent augmente régulièrement avec le temps dans la région sud (22°-34 °N). A mesure que l'on augmente en latitude dans les régions centrale et sud, la température de surface moyenne diminue significativement. En réponse aux phénomènes ENSO, mais aussi en raison du changement de régime de 1976, la température de surface augmente rapidement au large de la Californie mais beaucoup plus lentement aux autres latitudes. Alors que la température de surface a augmenté tout le long de la côte durant les dernières décades, elle a diminué au large du 36 °N. Cette tendance longue au refroidissement au nord du système du courant californien est liée aux anomalies froides à grande échelle observées dans le Pacifique nord plutôt qu'à des changements de la direction locale des vents. C'est un ensemble de processus différents qui est responsable de la tendance au réchauffement le long de la côte. Il apparaît également que des combinaisons particulières d'advection dues au forçage du vent, au mélange et à l'échauffement direct provoquent, dans les zones côtières, des réponses régionales aux changements climatiques pouvant être très différentes. Ceci pourrait donc avoir des conséquences importantes sur les populations d'espèces marines dans les écosystèmes d'upwellings côtiers.

INTRODUCTION

In eastern boundary current (EBC) systems, the physical environment is rarely uniform in time. In addition to seasonal and higher frequency variations, ENSOs and other perturbations produce profound anomalies in the atmosphere and ocean on interannual to decadal and century time scales. Analogously, EBCs appear to be spatially heterogeneous. Each system can be separated into several discrete regions, dominated by different physical processes, and presumably different biological structure. These regions may be separated by sharp gradients in physical forcing and characteristics, or by broad transition zones that extend over several degrees of latitude. It is expected that environmental variability in an EBC will impact its ecosystem's components, and may lead to perturbations in plankton and fish abundance, biomass and distribution. The timing of seasonal cycles in each region, as well as the timing and intensity of large-scale events (e.g. ENSOs), may not be coherent throughout an ecosystem.

To understand better how EBC ecosystems might respond to climate change, it is critical to describe their primary scales of spatial and temporal variability, and discern the dynamics responsible for this variance, rather than treat EBCs as spatially homogeneous systems or use seasonally-averaged data to describe their climatology. This background is essential if scientists are to address the likely impact of climate change scenarios on ecosystem structure and the distribution of its populations.

The objective of this paper is to describe the temporal variability in the spatial texture of the California Current System (CCS), a major EBC system, to provide a base from which to evaluate the effect of climate variability in the environment on fisheries - in the recent past, at present, and for the future. Specifically, we will describe the patterns of variability that have occurred over the past 45 years (1946-1990) in the monthly-averaged wind stress and sea surface temperature (SST) fields of the CCS, using state-space statistical models (Schwing and Mendelssohn, this vol.) to separate a non-linear, non-parametric trend for each series from seasonal and other higher frequency variance. It is our hope that the results described here will encourage researchers to look for analogous spatial and temporal patterns in climate variability in other EBCs and relate this variability to fluctuations in marine populations.

1. METHODS

The environmental data used to generate the monthly-averaged time series analyzed here were obtained from a variety of sources. The primary data base was the Comprehensive Ocean-Atmosphere Data Set (COADS). The COADS contains almost 100 million reports of ocean surface conditions, mostly taken by ships-of-opportunity. The data have been collected, quality-controlled and put into common formats and units (Slutz *et al.*, 1985; Woodruff *et al.*, 1987). Data were extracted using the CD-Rom-based version of COADS and the CODE extraction program described in Mendelssohn and Roy (1996). The CD-Rom version contains Release 1 of COADS for the period 1854-1979 and the Interim release for 1980-1990, in CMR5 format.

Only wind data marked as estimated or unknown were used in forming the mean series, to avoid as much as possible the known bias in the data due to an increase in the use of anemometer-wind measurements (Cardone *et al.*, 1990; Isemer, 1992; Wu and Newell, 1992). All COADS observations outside of the wide interval (see Slutz *et al.*, 1985, page D6) were excluded from the summaries as well. Poleward wind pseudo-stress, henceforth referred to as wind stress, was derived by squaring the northward wind component from each record included in the extraction. Spatial regions approximately two-degree latitude by four-degree longitude were defined based on a combination of ecological and oceanographic features as well as on data density, and monthly mean time series of wind stress and sea surface temperature (SST) were calculated for each region (Fig. 1, Table 1). These geographic boxes are referred to in terms of their central latitude (e.g. 23°N refers to the 22-24°N COADS box). The time period of extraction is 1946-1990.

The parameterization of wind stress used here is one of several possibilities found in the scientific literature. It was applied because only the time series of the north wind components were available initially. Winds along the west coast are oriented predominantly north-south. Follow-up analyses using the wind total vector, as well as other stress parameterizations, provide very similar results, suggesting the north wind series described here qualitatively represent the variability in the coastal wind field over the past half-century.

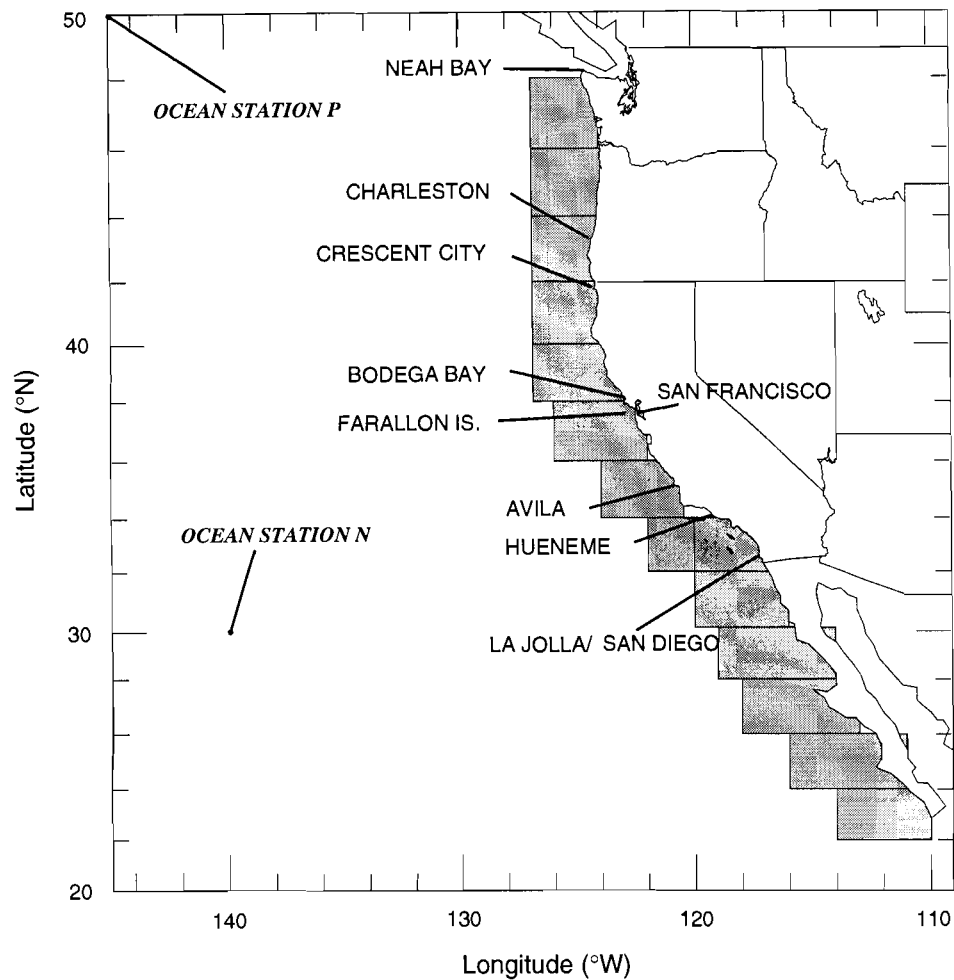


Fig. 1: Locations of COADS 2° boxes, shown as shaded boxes, and coastal stations from which monthly time series were generated. Locations of Ocean Stations P and N also are shown.

Shore-based monthly-averaged sea surface temperature (SST) time series were derived from daily observations made by volunteers, which are sent to the Marine Life Research Group, Scripps Institution of Oceanography (Walker *et al.*, 1993). SSTs were reported to the nearest 0.1°C at most sites and are accurate to about $\pm 0.2^\circ\text{C}$. The number of daily samples per month varied from 15-20/month (and as little as 10/month during winter months) at some of the northern stations (e.g. Farallon, Crescent City), to nearly complete coverage (e.g., La Jolla) (Skillman, 1993). The locations of the primary stations are shown in Figure 1 and Table 1.

COADS BOX (°N)	COADS LAT (°N)	COADS LONG (°W)	SHORE & OCEAN STATIONS (°N)	SST
47	46-48	124 - 127	Neah Bay (48°22')	1935-1992
45	44-46	123.5- 127	—	—
43	42-44	124 - 127	Charleston (43°21')	1966-1992
41	40-42	123 - 127	Crescent City (41°45')	1933-1992
39	38-40	122 - 127	Bodega Bay (38°19')	1957-1992
37	36-38	122 - 126	Farallon (37°25')	1925-1992
35	34-36	120.5- 124	Avila (35°10')	1945-1992
33	32-34	120 - 122	—	—
BIGHT	32-34	116 - 120	Hueneme (34°09')	1919-1987
			La Jolla (32°52')	1916-1992
31	30-32	116 - 120	—	—
29	28-30	114 - 119	—	—
27	26-28	113 - 118	—	—
25	24-26	111 - 116	—	—
23	22-24	110 - 114	—	—
—	—	—	Station P (50°N,145°W)	1950-1992
—	—	—	Station N (30°N,140°W)	1954-1974

Table 1: Dimensions of COADS boxes containing derived monthly averaged equatorward wind stress and SST (for period 1946-1990), and selected shore stations within the COADS boxes. Dates for monthly averaged time series of SST, salinity and sea level shown.

To estimate a time-varying (i.e. non-stationary) trend component for each monthly-averaged time series, we assume that each monthly average $y(t)$ is the sum of four components

$$y(t) = T(t) + S(t) + I(t) + e(t), t=1, T(1)$$

where, at time t , $T(t)$ is the unobserved time-dependent mean-level (trend), $S(t)$ is the seasonal component, $I(t)$ is the irregular term (stationary but autocorrelated), and $e(t)$ is the stationary uncorrelated component, which can be viewed as 'observation' or 'measurement' error. A non-parametric and non-linear trend is estimated for the monthly-averaged time series using a state-space model solved by using a combination of the Kalman filter and maximum likelihood methods (Kitagawa and Gersch, 1984, 1988). The trend term in Equation 1 can be viewed as an unknown function of time, and parameterized as

$$\nabla^k T(t) \sim N(0, \sigma_T^2). (2)$$

For $k = 1$ and $\sigma_T^2 = 0$, Equation 2 reduces to a linear fit; i.e. $T(t) = a + bt$, rather than the discrete equivalent of a k -th order smoothing spline. Figures 2 and 3 show examples of observed time series of wind and SST, respectively, along with their respective trends from the state-space models. The models work much better in accounting for SST variability; the difference between the SST trend and the residual of the observed, less the seasonal and AR series, (equal to the trend plus model error) is negligible. The errors in the wind stress models are higher, presumably because the response time of SST to atmospheric forcing acts to 'smooth' month-to-month variability occurring in wind forcing. These examples also demonstrate that variability in long-term trends is small relative to that in the seasonal cycles of wind stress and SST, pointing to the need for a method that will extract long-term variability for analysis of climate change. Schwing and Mendelsohn (this vol.) and Durand and Mendelsohn (this vol.) discuss in detail the statistical techniques applied here.

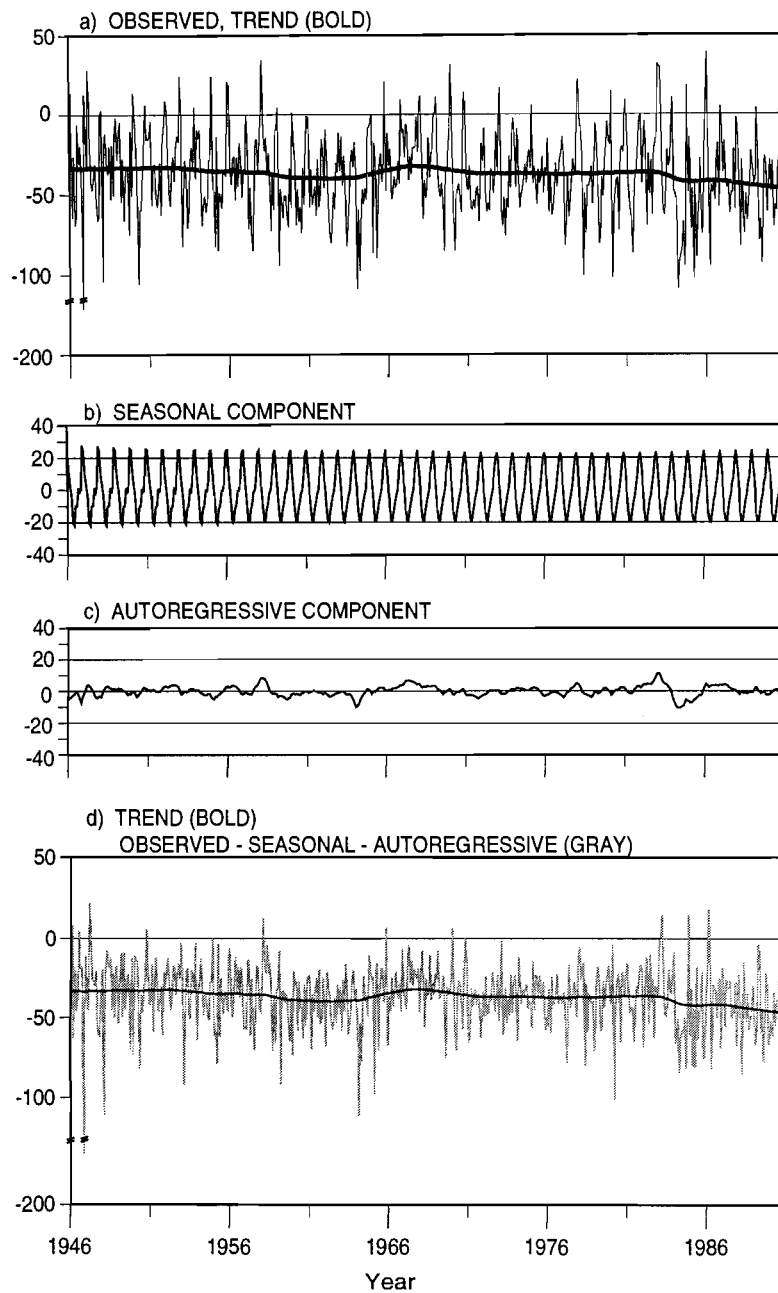


Fig. 2: Comparison of COADS-37°N (36-38°N) poleward wind stress monthly observations to model results, for period 1946-90. a) overlay of trend model component (bold line) and observed monthly series; b) seasonal model component; c) autoregressive (AR) model component; d) overlay of trend model component (bold line) and observed series minus seasonal and AR model components (gray line). The y-axes of panels a) and d) have been condensed to ease presentation of one large negative observation.

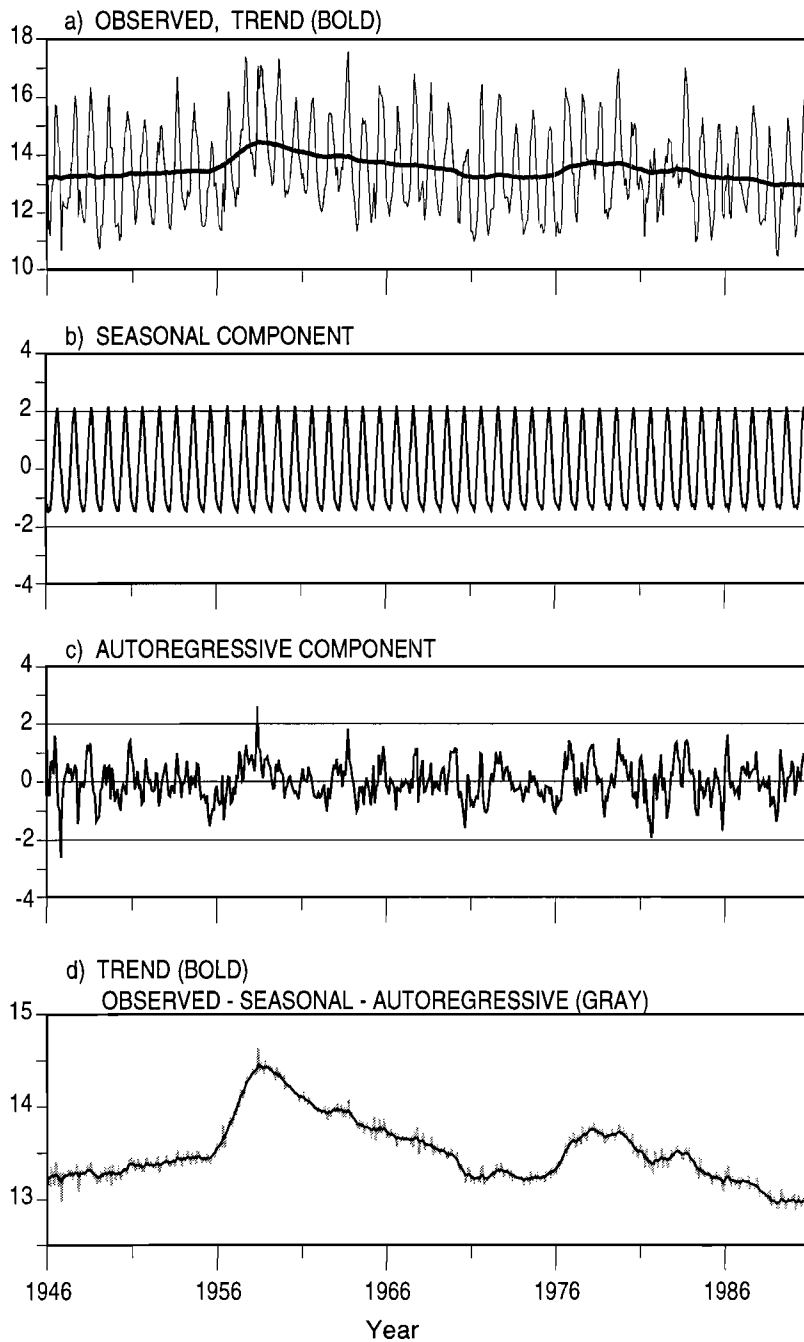


Fig. 3: Comparison of COADS 37°N (36-38°N) SST monthly observations to model results, for period 1946-90. a) overlay of trend model component (bold line) and observed monthly series; b) seasonal model component; c) autoregressive (AR) model component; d) overlay of trend model component (bold line) and observed series minus seasonal and AR model components (gray line). The y-axis of panel D has been expanded for clarity.

2. RESULTS

Time series of poleward wind stress trends for the COADS 2° boxes display the spatial and temporal variability of the CCS wind field (Fig. 4). The wind separates into three distinct geographical regions; $22\text{-}32^\circ\text{N}$ (south), $32\text{-}40^\circ\text{N}$ (central), and $42\text{-}48^\circ\text{N}$ (northern), based on a visual comparison of the time series, and the clustering of statistical correlations between the series (Table 2). Wind stress trends in the southern region (dashed-dotted lines) became increasingly equatorward (negative) over time in a relatively monotonic pattern, as noted by the highly linear fits to the series (Table 3). Stress also strengthened from 22° to 30° , but was weaker in the southern California Bight; local maximum equatorward stress was seen over $26\text{-}30^\circ\text{N}$. The Bight featured weaker stress and more variability on 5-10 year scales, relative to adjacent boxes, and is weakly correlated with the other wind time series in the CCS, particularly those off central California.

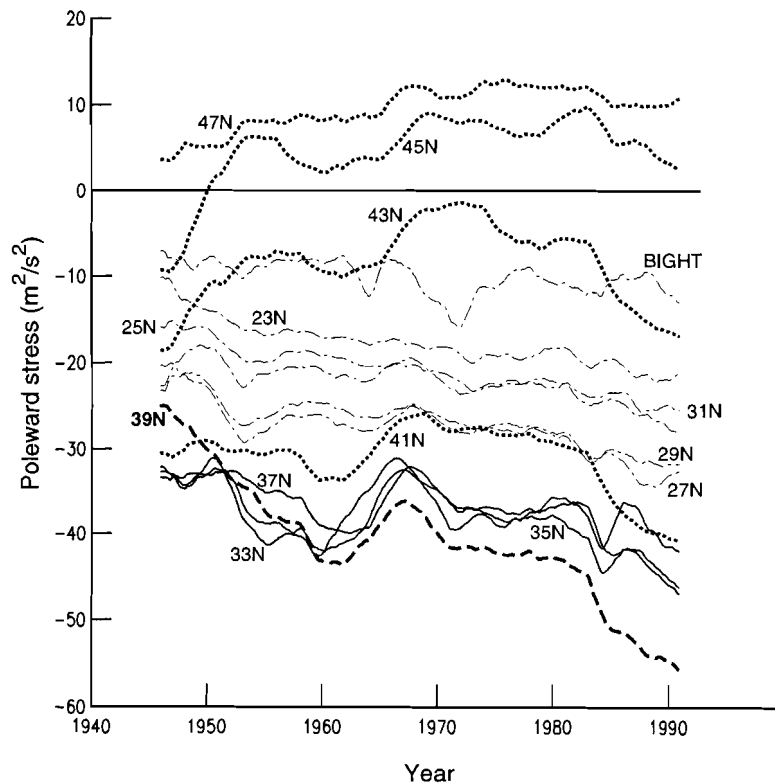


Fig. 4: Time series of poleward wind stress trends for COADS boxes. Dashed-dotted lines represent time series from the southern region ($22\text{-}32^\circ\text{N}$). Solid lines represent time series from the central region ($32\text{-}40^\circ\text{N}$). Bold dotted lines represent time series from the northern region ($40\text{-}48^\circ\text{N}$). Bold dashed line represents the 39°N time series.

	23N	25N	27N	29N	31N	BIGHT	33N	35N	37N	39N	41N	43N	45N	47N
47N	-0.80	-0.73	-0.57	-0.59	-0.51	-0.59	-0.34	-0.36	-0.36	-0.62	.05	.60	.84	
45N	-0.71	-0.60	-0.49	-0.61	-0.37	-0.56	-0.29	-0.25	-0.17	-0.53	.13	.73		.94
43N	-0.17	-0.01	.17	.01	.16	-0.39	.03	.28	.37	.08	.71		.76	.59
41N	.49	.59	.72	.65	.68	.08	.58	.83	.87	.71		.41	.81	.83
39N	.93	.93	.91	.89	.81	.47	.65	.86	.90		.82	.24	.72	.81
37N	.77	.81	.84	.80	.84	.37	.71	.93		.90	.90	.52	.84	.83
35N	.72	.75	.79	.82	.80	.31	.87		.84	.61	.73	.76	.85	.77
33N	.59	.57	.59	.68	.69	.35		.75	.39	.12	.28	.73	.51	.45
BIGHT	.61	.62	.51	.55	.60		.98	.74	.41	.13	.22	.90	.61	.49
31N	.80	.88	.92	.88		.98	.89	.78	.43	.11	.28	.90	.63	.50
29N	.90	.91	.94		.97	.95	.84	.66	.27	-0.08	.15	.90	.52	.35
27N	.90	.96		.98	.96	.95	.79	.67	.33	.00	.19	.95	.59	.41
25N	.96		.96	.93	.94	.93	.78	.77	.49	.22	.38	.97	.76	.62
23N		.97	.87	.83	.88	.87	.72	.77	.56	.35	.46	.91	.82	.73

Table 2: Correlation matrix for COADS 2° box trend time series. Upper-left half of matrix shows correlations between poleward wind stress series. Lower-right half shows correlations between SST series. Clusters of correlation values in bold denote subjective groupings of highly coherent series in three geographic regions. Spaces between rows and columns separate regions within CCS, based on subjective examination of time series. The 0.01 level of significance is 0.11 (n=540).

The central region (solid lines) displayed the strongest equatorward stress in the CCS (Fig. 4). Stress trends became increasingly equatorward over time (Table 3), but exhibited much more interannual variation compared to the southern region. The stress series at these latitudes are less correlated with those in the other regions as a result of this interannual variability (Table 2). A period of stronger than normal stress in the 1950s was followed by a period of decreasing equatorward stress in the mid-1960s. The center of this region (39°N, bold dashed line in Fig. 4) featured the greatest change over time (Table 3), shifting from the site of the region's weakest stress in the 1960's to strongest stress in the 1980's. While stress in the Bight appears relatively uncoupled with this region (Fig. 4, Table 2), winds immediately offshore of the Bight (33°N in Fig. 4) are similar to the central region's stress series.

In contrast to wind stress off California and Baja, the region north of 44°N featured a mean poleward stress that strengthened over time (Fig. 4, Table 3). These series are negatively correlated with virtually the rest of the CCS, due to their opposing series-long trend. 40-44°N was a transition area between the central and northern regions; equatorward stress decreased rapidly north of 40°N. In about 1976 the 43°N COADS series shifted from the pattern seen in the northern region to that of the central region. This results in the 43°N winds being poorly correlated with most of the other stress series.

Two temporal phenomena are notable for their absence in the stress trend series. ENSO events (e.g. 1957, 1983) are not apparent in the series. Instead the model allocated their variance into the AR series (Fig. 2c), and model error (difference in gray and black lines in Fig. 2d), presumably because the wind field responds rapidly to a developing and decaying ENSO.

The well-documented regime shift in 1976 (Trenberth, 1990; Ebbesmeyer *et al.*, 1991; Miller *et al.*, 1994, Trenberth and Hurrell, 1994) is not seen in the wind trends either, despite its clear presence in north Pacific atmospheric pressure indices. A likely possibility is that the CCS is out of the region where winds were directly affected by the intensification of the Aleutian Low beginning in 1976. However a substantial increase in equatorward stress did occur in about 1983 in the central region and north to about 44°N. One interpretation of this intensification is that the transition zone between the central and northern regions has broadened south; another is that the area off northern California and Oregon developed its own distinct wind regime after 1983. In either case, the net effect is that the alongshore gradient in poleward stress has strengthened greatly over the last 45 years.

	23N	25N	27N	29N	31N	BIGHT	33N	35N	37N	39N	41N	43N	45N	47N
Stress:SST	-.26	-.41	-.61	-.60	-.34	.07	-.03	-.23	.16	.41	.37	-.04	.16	-.21
Stress:Time	-.92	-.95	-.89	-.80	-.80	-.55	-.33	-.63	-.73	-.89	-.41	.10	.61	.77
slope	-17.7	-21.7	-21.3	-16.5	-10.7	-7.9	-7.9	-17.0	-19.3	-48.3	-11.9	3.3	19.4	14.7
SST:Time	.23	.43	.63	.66	.49	.48	.34	.09	-.33	-.63	-.38	.48	-.13	-.37
slope	3.4	8.9	16.8	16.4	12.6	11.2	8.3	1.5	-8.7	-22.9	-12.6	9.5	-2.3	-7.8

Table 3: Correlation matrix for COADS 2° box trend time series. First line shows correlations between stress and SST series, for each COADS box. Second and third lines show correlation between COADS stress and time, and slope of linear fit between stress and time (linear rate of change, 10^{-2} m²/s²/year), respectively. Positive (negative) sign denotes linear trend for increasing poleward (equatorward) stress. Fourth and fifth lines show correlation between SST and time, and slope of linear fit between SST and time (linear rate of change, 10^{-3} °C/year), respectively. Positive (negative) sign denotes warming (cooling) trend. Spaces between columns separate three geographic regions within CCS, based on subjective examination of time series. The 0.11 level of significance is 0.11 (n=540).

Contours of COADS poleward wind stress trend anomalies, relative to the long-term mean at each latitude, reveal additional temporal and spatial patterns in the wind field (Fig. 5). For reference, the zero contour of the stress trends (dashed line) is included. Prior to the mid-1950s, stress anomalies were negative (more equatorward) north of 40°N and positive (less equatorward) south of 40°N. A particularly strong spatial contrast occurs in the 38-44°N region at the beginning of the series. A period of negative stress anomalies north of 30°N began near the onset of the 1957 ENSO and continued into the early 1960s, contrasting with a contemporaneous period of weak positive anomalies south of 30°N. Stress was anomalously strong throughout the entire CCS from about 1964 to 1970. Since 1970, anomalies have become increasingly negative (more equatorward) south of 40°N, and negative at higher latitudes since about 1983.

The COADS SST trends separate visually (Fig. 6) and statistically (Tables 2 and 3) into essentially the same geographic regions as wind stress. For example, the relatively poor correlation of SST series off northern California with those in the south (Table 2) imply a different pattern of interannual ocean variability in the central CCS. However SST is more correlated in space than wind stress on interannual (1-5 year) scales (Fig. 6). SST decreased consistently with latitude from about 22°N to 40°N (fine lines), coincident with a region of equatorward wind stress. SST north of 40°N (bold lines) was nearly uniform with latitude, an area where stress was either generally poleward or becoming less equatorward over time. While ENSO wind

events are relatively ephemeral, and thus are relegated to the model AR term, warmer conditions associated with ENSOs are obvious in the SST trend series, and appear to gradually dissipate long after the ENSO atmospheric signal (compare also Fig. 2 and 3). However some ENSO signals appear in the SST AR component as well (Fig. 3c). Interannual variations in the series (e.g. the 1957 ENSO event) are greatest off central and southern California (Fig. 6). In contrast to the 1957 event, the 1982 ENSO is reflected in SST as a smaller local maximum relative to adjacent years.

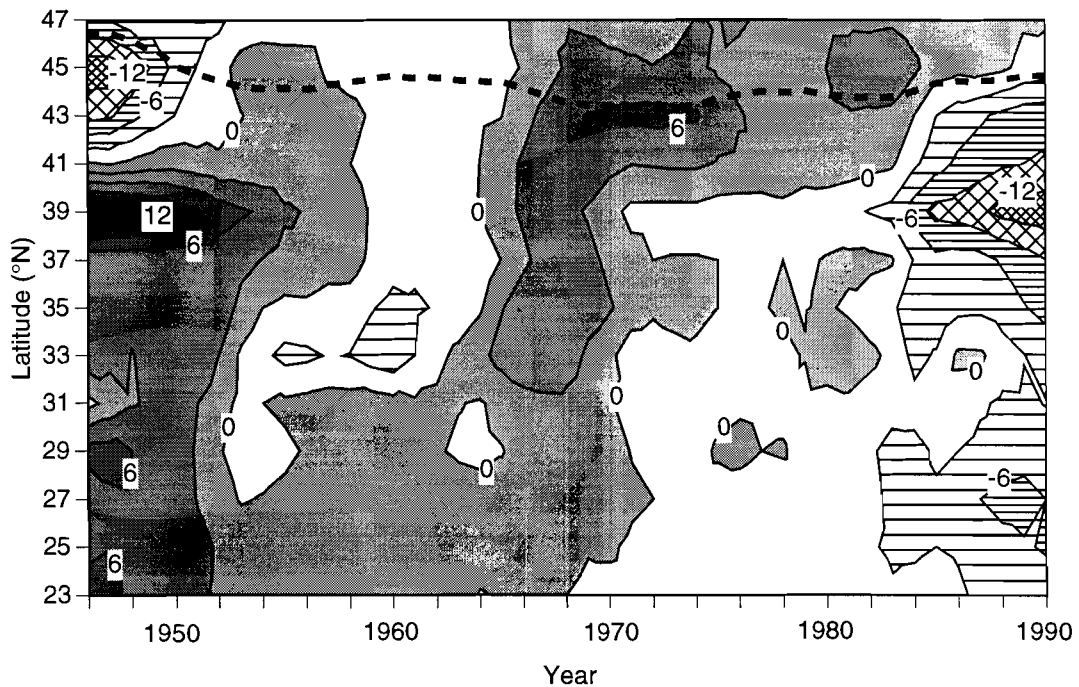


Fig. 5: Contours of poleward wind stress trend anomaly series for COADS boxes. Anomalies are with respect to series means for each 2° box. Shading denotes positive anomalies; hatching denotes negative anomalies. Contour interval is $3 \text{ m}^2/\text{s}^2$. Broken line denotes location of zero wind stress.

The obvious warming beginning in 1976, a climate shift not reflected in stress, suggests that decadal-scale SST variability in the CCS is controlled by the large-scale pressure and wind fields, rather than local wind forcing. The shift in 1976 rivals the degree of warming associated with the 1957 ENSO. Since the mid-1980s, SST south of 32°N increased slightly, but cooled substantially north of 34°N . The series-length linear tendencies (linear regressions of time series, Table 3) are significantly positive (increasing SST) south of 34°N and in the 43°N box, but significantly negative north of 36°N (save 43°N). The alongshore SST gradient off southern California strengthened over time (Fig. 6). Simultaneously the SST gradient along northern California decreased. SST at 39°N (fine broken line) decreased gradually over time, cooling to values seen at higher latitudes. At the same time, 43°N SST (bold broken line) warmed relative to nearby boxes. The convergence of SST in the $38\text{--}42^\circ\text{N}$ region coincides geographically with the strong temporal intensification in stress at these latitudes (Fig. 4 and 5).

Contours of SST trend anomaly series for the COADS 2° boxes (Fig. 7) reinforce the idea that decadal-scale variability in SST is generally coherent throughout the CCS. Anomalously cool periods prior to 1956 and during 1968-1977 contrast with warm events during 1956-1968 (following the 1957 ENSO) and since 1977 (following the 1976 regime shift). These warm and cool periods are not coherent with any periods of anomalous wind stress (Fig. 5). Years featuring ENSO events were characterized by rapid warming. Warm conditions remained several years after the 1957 event. However the warming and cooling associated with the 1983 ENSO was more symmetric. Since about 1985, conditions have remained warm south of 34°N, but have been cooler in the north. The strong series-long cooling trend at 39°N (Table 3) can be seen in the anomalies (particularly when contrasted with regions to the south), which corresponds to strengthening equatorward stress

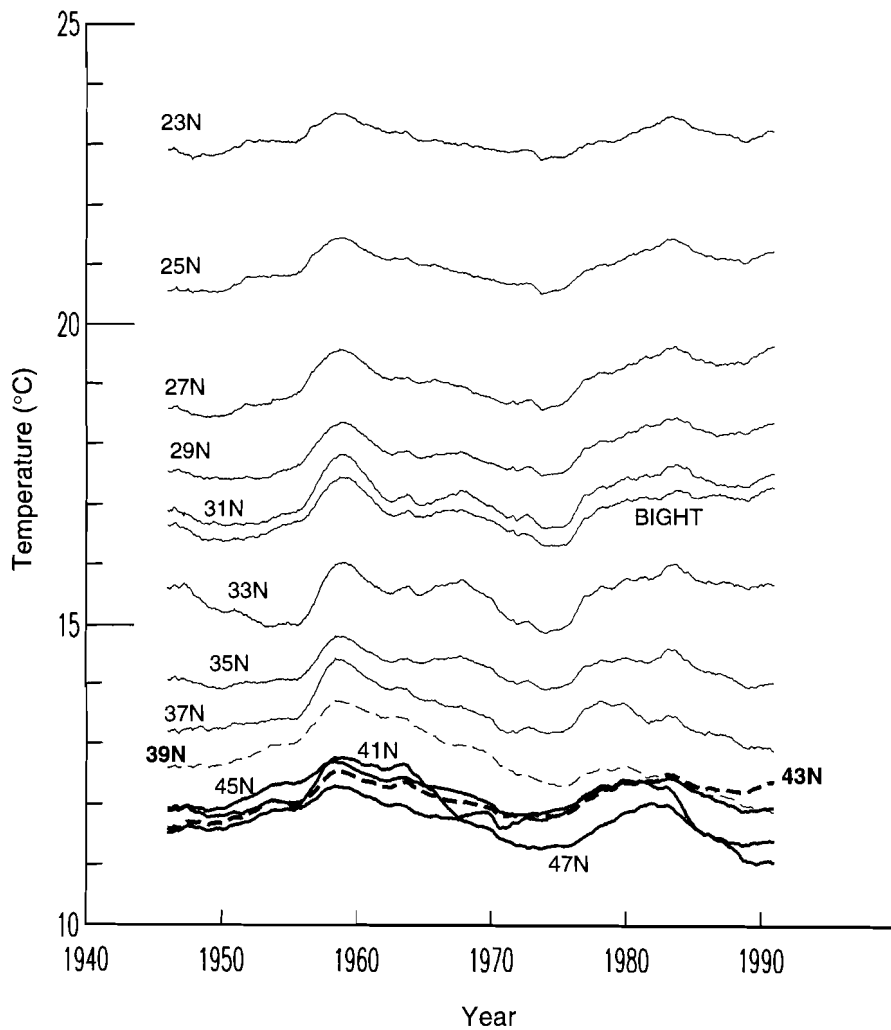


Fig. 6: Time series of SST trends for COADS boxes. Fine lines denote time series south of 40°N. Bold lines denote time series north of 40°N. Fine and bold broken lines denote time series for 39°N and 43°N COADS boxes, respectively.

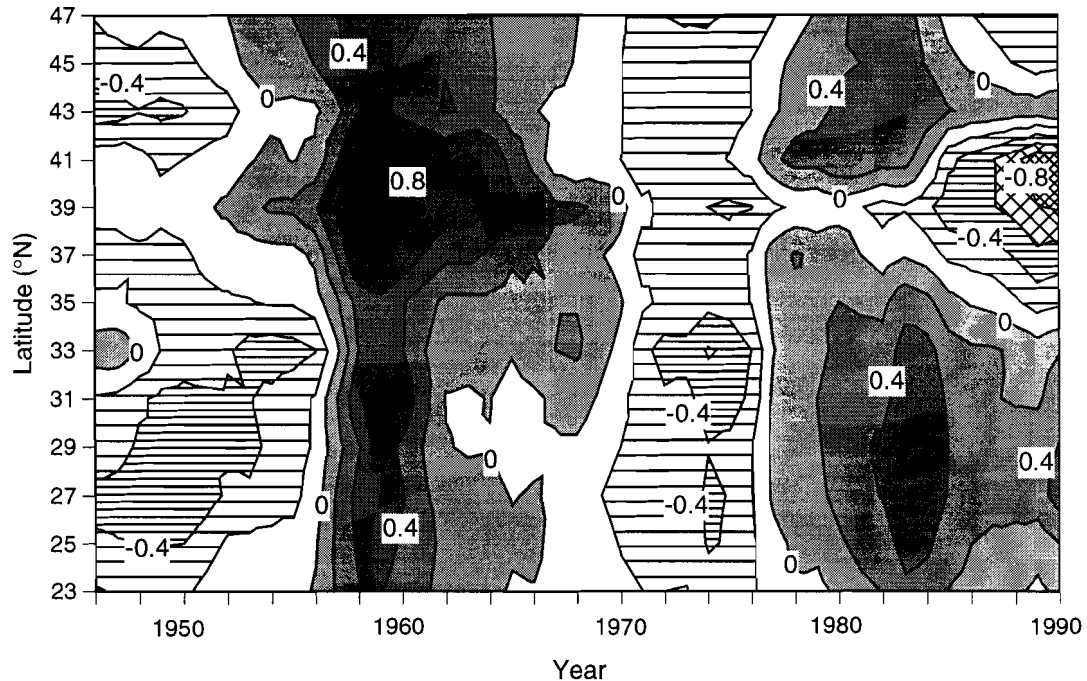


Fig. 7: Contours of SST trend anomaly series for COADS boxes ($^{\circ}\text{C}$). Anomalies are with respect to series means for each 2° box. Shading denotes positive anomalies; hatching denotes negative anomalies. Contour interval is 0.2°C .

(Fig. 4 and 5). As mentioned earlier, however, the SST (Fig. 7) and wind stress (Fig. 5) anomalies do not agree otherwise, suggesting that local winds are not the primary factor controlling decadal-scale temperature variations in the CCS.

Shore-based SST trend time series along the western North American coast (Fig. 8), derived with the state-space model, provide an independent assessment of SST variability, extended in space and time. These series also allow a finer (along- and across-shore) spatial scale look at temporal variability. As with the COADS SSTs (Fig. 6 and 7), the shore series demonstrate well-defined latitudinal regimes in ocean temperature on decadal scales. ENSO events (Quinn *et al.*, 1987) are shown by the shaded vertical lines in Fig. 8; their large-scale warming influence is seen. Coastal warming associated with ENSOs was greatest along central California. The SST signal of some ENSO events (e.g., 1972-1973) appears to be weak and constrained to southern stations.

The shore series (Fig. 8) show that many of the temporal features of CCS SST extend north into the Gulf of Alaska and well offshore (Ocean Stations P and N). However there also are obvious regional differences between the CCS and coastal locations off British Columbia and Alaska, particularly during ENSO events and on decadal scales. Numerous other regional differences in the trends are evident. Most coastal sites feature series-long warming trends that are highly non-linear and display considerable variability on annual-to-decadal scales. Most series have 10-20 year periods of relatively level temperature, followed by similar periods of rapid temperature increase. Some series have multi-year periods of decreasing temperature. Higher latitude sites have a well-defined cycle of about 20 years, which Royer (1993) attributes to the 18.6-year tide.

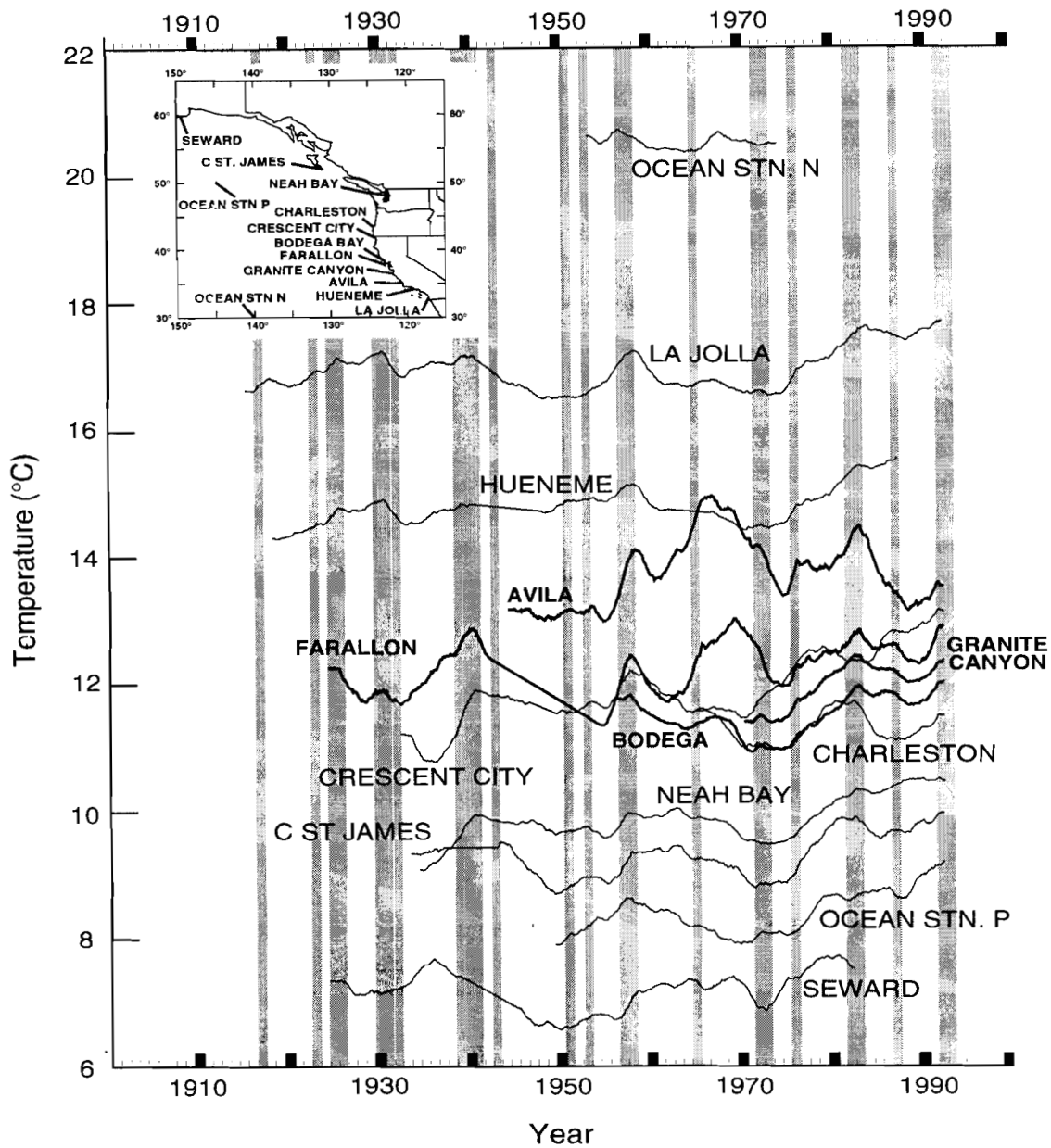


Fig. 8: Trend time series of SST ($^{\circ}\text{C}$) from several coastal sites along North American west coast (locations shown on map in inset). Time series for Ocean Stations P and N also shown. Bold lines denote time series from central California locations. Shaded vertical bars denote ENSO periods, based on Quinn et al. (1987).

The shifts to a cool regime in 1941 and to a warm regime in 1976 (MacCall and Prager, 1988) are evident in the shore series as well. The 1976 shift occurred rapidly along southern California. However it was less dramatic and occurred over several years at more northern sites, thus appearing more as a gradual warming. The 1941 transition is more difficult to document, but appears less dramatic relative to the 1976 shift. The regime shift concept may be valid for some regions (e.g., southern California), but displays a considerable degree of inter-regional difference.

In addition to alongshore differences in CCS SST, a comparison of selected COADS SST and nearby coastal SST trend time series (Fig. 9) suggests there also are significant differences between nearshore and offshore temperature trends. SST in the Southern California Bight agrees well with shore-based SST at La Jolla. Further north, however, offshore and shore SST series at corresponding latitudes are poorly correlated. Although the COADS SST trends cooled over time north of about 36°N, the coastal SST trend series warmed over time along the entire U.S. west coast. Shore series accentuate interannual-to-decadal changes as well. Like the COADS SSTs, shore SST trend series are poorly correlated with COADS poleward wind stress.

A particularly interesting feature is the close positive correlation between Crescent City and adjacent COADS SST from about 1970-1983, followed by an apparent inverse relationship since. The adjacent wind stress also appears to be negatively correlated with shore SST, and positively correlated with COADS SST, since 1983. Another intriguing relationship is the close correspondence between an approximately five-year period of weakening equatorward stress and warming shore SST in the late 1960s, centered along central California (e.g., Farallon, Avila). This was followed by a similar length period when wind stress and SST returned to values seen in the early 1960s. This warming/cooling event is not reflected in the adjacent COADS boxes. Both of these events attest to the considerable decadal-scale variability inherent in the CCS, which is not always associated with ENSO events, and merit a closer analysis. The results also suggest the CCS may experience a substantial degree of cross-shelf variability as well.

Although the COADS observations do not have sufficient wide-spread density of coverage to produce monthly time series at 2° resolution for the greater northeast Pacific, or to resolve the spatial variability of the CCS on finer scales, we can examine spatial differences in the area's SST and wind fields at a 1° resolution by averaging the observations for two separate decades (1966-1975 and 1977-1986) to contrast conditions prior to and after the 1976 climate shift. Differences in SST between these periods (Fig. 10) corroborates the monthly time series' patterns. SST in recent years south of Oregon has been warmer (gray shades) in, and well offshore of, the CCS. The region north of California also appears to have been warmer at the coast and to about 150 km offshore after 1976. However SST in 1977-1986 in an offshore area off Oregon and Washington was cooler (hatched areas) relative to the earlier period. A closer analysis of these differences by season (not shown) suggests the cool anomaly in the northern CCS is connected to a much larger cool anomaly that covers much of the central North Pacific. Furthermore the eastern edge of this large cool anomaly moves eastward from February to September. Negative SST anomalies nearly reach the coast of Oregon and Washington by summer.

Like the relationship between the wind and SST time series, however, the distribution of SST anomalies over the northeast Pacific since 1976 is not coherent with changes in local wind stress or mixing. For example, most of the CCS south of 40°N, which was warmer in 1977-1986 relative to 1966-1975, featured greater equatorward stress and turbulent wind mixing during the latter period, which should lead to cooler SST. Thus it does not appear that interannual to decadal changes in SST, and more generally upper ocean conditions, are dominated by climate shifts in local wind forcing. We conclude that a complex interaction of local and remote Ekman advection, wind mixing and direct heating is responsible for the long-term fluctuations in SST in the CCS and northeast Pacific. Regional-scale differences in the relative importance of the mechanisms responsible for decadal-scale climate change in the northeastern Pacific is subject of ongoing research.

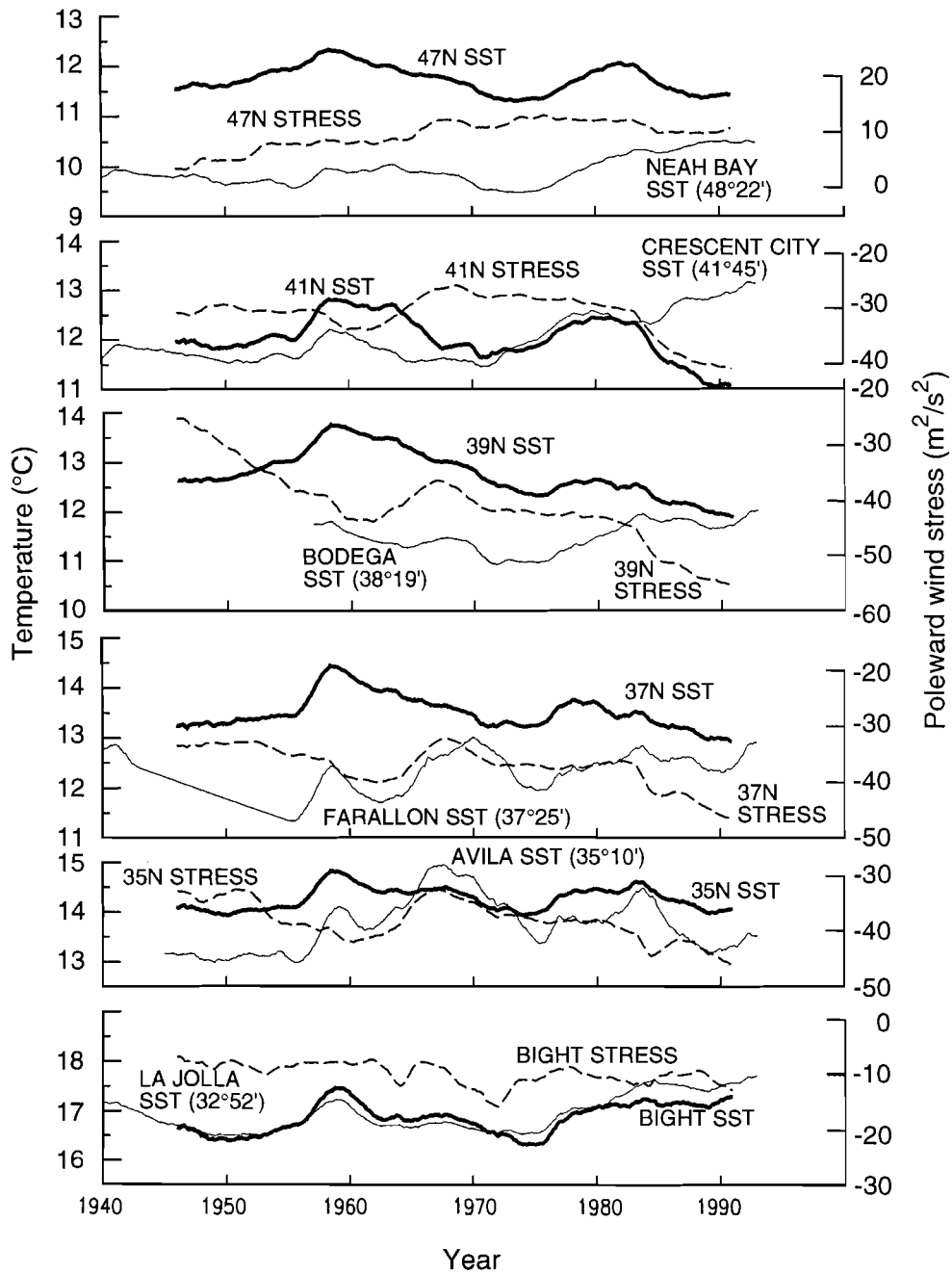


Fig. 9: Trend time series of COADS SST and poleward wind stress, compared with selected nearby coastal SST series. Bold solid lines represent COADS SST series. Fine solid lines represent coastal SST series. Broken lines represent wind stress series. Location of the time series are shown in each plot.

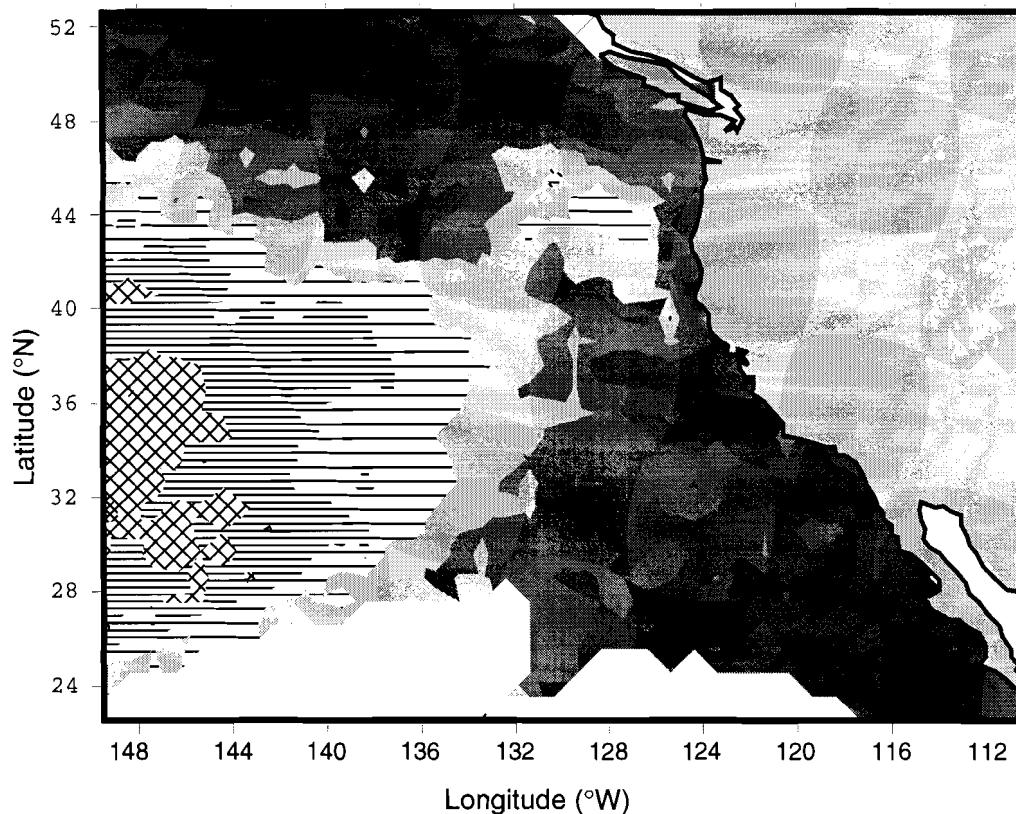


Fig. 10: Difference map of SST for northeast Pacific comparing annual means in 1° by 1° boxes from two ten-year periods (1977-1986 less 1966-1975). Positive values (shaded areas) denote relatively warmer SST in 1977-1986; negative values (hatched areas) denote relatively cooler SST in 1977-1986. Contour interval is 0.25°C . Range of contours is -0.75 to $+1.25^\circ\text{C}$.

3. DISCUSSION

The different regions of the CCS and the likely relationships between wind forcing and SST on long time scales are illustrated in Figure 11. The Figure shows the slope (\pm 99% confidence intervals) of a linear fit to poleward stress and SST trend time series in each COADS box; i.e., the linear tendency of each series (Table 3). A statistically significant tendency of increasing equatorward stress coincides with a cooling trend in much of the central region (34 - 42°N). A reasonable explanation for this pattern is that increasing stress leads to greater offshore Ekman transport and more coastal

upwelling, which cools the surface waters of this portion of the California Current. This region coincides with the geographic range of the upwelling maxima along the west coast (Parrish *et al.*, 1981). However shore-based SSTs feature a long-term warming tendency, countering the argument for greater coastal upwelling. A more likely explanation is that SST in the CCS is responding to large-scale atmospheric forcing that is changing in a way that leads to cooler surface conditions in the CCS at these latitudes. It is also possible that an increase in the positive wind curl occurring off northern California (Bakun and Nelson, 1991) could have accompanied the greater equatorward stress, and led to cooler SST through intensified Ekman pumping. Increased equatorward stress also would contribute to cooler SST through greater turbulent mixing of the upper ocean, and may be associated with increased southward transport of cool water by the California Current.

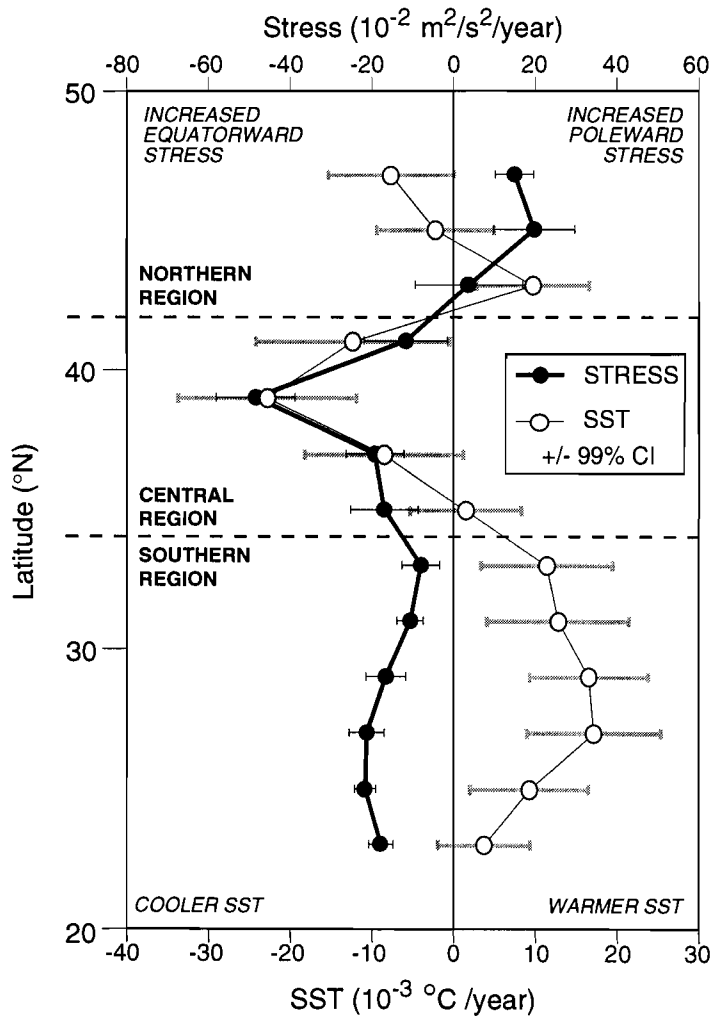


Fig. 11: Slopes of a linear fit to COADS poleward stress (solid circles) and SST (open circles) time series. 99% confidence intervals shown by horizontal bars (gray for stress, black for SST). Dashed lines denote boundaries of three geographic regions within CCS.

Outside of the central region the trends in stress and SST are negatively correlated. Increasing equatorward stress coincides with warming SST south of 34°N, while greater poleward stress accompanies a cooling trend north of 44°N. The cooler SSTs off Oregon and Washington may be due to greater wind mixing. Greater poleward stress could be linked to a larger (gyre) scale pattern in atmospheric circulation, such as the documented intensification of the Aleutian Low, which could lead to fundamental changes in the region's ocean circulation. However, a more rapid cyclonic transport of the Subarctic Current, typically associated with a deeper low, should increase SST. An examination of long-term changes in Ekman divergence due to variability in the wind field is beyond the scope of this study, but this could impact SST as well. We suspect that the transitional region between the Subarctic and California Currents could be extending southward, based on the expanding region of spatially uniform SST (Fig. 6). This would be consistent with cooler SSTs. We also believe, based on preliminary analysis of data from the entire north Pacific, that major shifts in the magnitude, position, and composition of the West Wind Drift feeding into these boundary currents may have changed over time. This is currently an active area of investigation.

The relationship between wind stress and SST in the southern region (22-34°N) is more difficult to explain. It is difficult to arrive at a scenario that is consistent with a long-term tendency for greater equatorward stress and warmer SST. Roemmich and McGowan (1995) present results for southern California consistent with those here, and speculate that increasing stratification over the last 45 years (due to an increasing heat flux from the atmosphere into the upper ocean) has more than compensated for greater wind stress, leading to shallower upwelling and a less effective 'cooling' from upwelling-favorable stress. Extending this idea to the regions farther north implies a different dynamical balance, such that the SST signal associated with greater stratification, a consequence of atmospheric warming, is overwhelmed by the role of changing wind patterns in driving more cool water into the surface layer of the CCS, through a combination of lateral advection from the central north Pacific, and upward movement by greater upwelling and vertical mixing.

In any case, it is apparent that over the last several decades surface waters in the CCS south of 34°N have experienced a different set of forcing conditions from those farther north. Not only are the tendencies of wind and SST different in these regions of the CCS (Fig. 11), but the spatially changing relationship between stress and SST implies that the primary mechanisms driving variability in SST, and probably the general circulation, on decadal time scales are fundamentally different in these various regions. It is not possible to develop a more firm conclusion about the mechanisms leading to these tendencies without a more thorough analysis of the temporal variability of wind vector fields over the north Pacific Ocean. However it is important to recognize that, over the last 50 years, wind and SST over the extent of the CCS has not fluctuated in a uniform manner (Tables 2 and 3). Thus using a single time series to represent climate variability in this ecosystem will give an incomplete, if not inaccurate, view of decadal changes in the CCS.

3.1. Ecological impacts of environmental variability

The temporal and spatial variability of the physical environment of the CCS described here must be considered when analyzing changes in the biological structure of this and other EBC ecosystems. Parrish *et al.* (1981) concluded that the larval assemblages and reproductive strategies of coastal fish species can be divided into regions that approximate the three areas defined from the long-term wind and SST patterns described here. Roemmich and McGowan (1995) have found that zooplankton biomass off southern California has decreased by 80% since 1951, while the surface layer has warmed by more than 1.5°C over the same time. They suggest this is due to an increase in stratification of the surface

layer, which has led to a shallower, hence lower nutrient, source of upwelling. However their observations are restricted to south of 34°N. The results reported here show that regional differences in environmental variability have existed in the CCS over the last five decades, therefore it is conceivable that analogous differences in biological productivity have occurred as well. Specifically Roemmich and McGowan (1995) note a correlation between declining zooplankton biomass and increasing near-surface temperature and stratification. If this model is correct, then could biomass be increasing in the northern portions of the CCS in association with the cooling tendencies of the COADS SST series? This cannot be immediately concluded, since SST variability may be linked with other variations (e.g., mixed layer depth) that influence production more directly.

It has been shown here that decadal-scale climate variability has considerable regional differences as well. Considerable evidence suggests that environmental conditions in the northeast Pacific in recent years can be described in terms of two climate phases, separated by a transition occurring in about 1976. From the early 1940s to about 1976, the eastern north Pacific was under the influence of increased equatorward stress (associated with a weaker than normal Aleutian Low in winter and a southward flowing jet stream), resulting in a cool pool of water along the entire North American west coast, and a warm pool in the central north Pacific. Beginning in 1976, the Aleutian Low deepened and shifted eastward each winter, which altered large-scale wind patterns, storm tracks and ocean currents. The resulting ocean thermal structure featured a warm water mass off central and southern California, but cooler water in the northern portion of the CCS and over much of the north subtropical Pacific (Fig. 10).

Anchovies were the dominant small pelagic in the CCS prior to 1976 (MacCall, 1986); however sardines have shown evidence of increasing biomass since (Barnes *et al.*, 1992). The decadal-scale fluctuations of the two dominant pelagic fishes appear to be associated with the larger scale variations in the CCS. From the mid-1920s to the early 1940s sardines dominated the entire CCS. This population collapsed during the 1950s and did not show any evidence of recovery until after the environmental shift in 1976; since then the population has shown a very large increase in its rate of growth (MacCall, 1979; Barnes *et al.*, 1992). Anchovies were not abundant in the southern region during the 1950s, but the population increased during the 1960s and reached a short term peak in the early 1970s. The California anchovy fishery peaked in 1975 and then declined sharply; whereas the Mexican anchovy fishery expanded after the mid-1970s peak in population, reached a maximum in 1981 and then totally collapsed in 1990 (Ainley *et al.*, 1993). These regional differences may be linked to spatial differences in the rate and magnitude of environmental changes. Based on the fishery information available since the 1920s, it appears that the CCS sardine stock rises during warm water periods and the southern region's anchovy stock rises during cold water periods. Conditions prior to the early 1940s, when sardines dominated the CCS, were similar to those since 1976. Baumgartner *et al.* (1992) analyzed anaerobic sediments off southern California and concluded that alternating dominance between sardines and anchovies has occurred back to at least 300 AD.

Although they are similar in many other respects, it appears that the anchovy and sardine utilize the CCS in quite different ways. Sardines, which are larger and more mobile than anchovies, migrate from the southern region into the central and northern regions for feeding and then return to the southern region to spawn. Anchovies, although they occur over the entire CCS, appear to be much more localized in their movements. They have separate genetic stocks in the northern and southern regions and, within the historical record, have not been very abundant in the central region. Thus it appears that anchovy populations may rise and fall based on differences in the environmental conditions in the three CCS regions; whereas the single sardine population may be affected by environmental conditions in any or all of the three CCS regions.

On shorter time scales, studies in the CCS demonstrate that biological production decreases dramatically during ENSO events (McGowan, 1985). ENSOs also are responsible for poor salmon survival off the northwest U.S. (Pearcy *et al.*, 1985), reduced recruitment, growth and condition of groundfish (Lenarz *et al.*, 1995), and dramatic range extensions for fish

(Radovich, 1961). While ENSOs have a large-scale influence, it is shown here that their relative environmental signal is highly variable over the length of the CCS ecosystem. In addition, individual ENSOs appear to have unique characteristics of timing, intensity and extent, superimposed on their canonical signal (1957, 1983). The corresponding biological effects presumably vary as well.

It is important to note that we observed substantial anomalies in the CCS that are unrelated to these well-defined climate events (e.g., 1965-1975, Fig. 9). Nevertheless, these periods of unusual environmental conditions are likely to have significant consequences for the ecosystem. 'Warm' years, when conditions off California are similar to those during ENSO events despite the absence of an equatorial ENSO signal, are linked to poor recruitment of central California rockfish, while 'cool' years feature enhanced recruitment (S.V. Ralston, Tiburon, NMFS, pers. comm.). Extreme year classes of several species of fish over large geographical areas tend to occur in association with unusual environmental conditions (Hollowed and Wooster, 1992).

The results presented here clearly demonstrate the highly variable nature of the CCS environment in time and space, and argue against oversimplifying EBC climate change as a constant linear trend, or in terms of the climate record from a single location. The distinct latitudinal regionalization and cross-shelf variability of the CCS wind and SST fields has key implications for fisheries. For example, which time series or regions are more important in terms of defining a stock's environment? Regional differences also mean that widespread stocks, or stocks that are highly migratory over their life history, face a spatially heterogeneous changing climate. Widespread stocks also may display a very different long-term variability from species whose domain is limited to the homogeneous regions of the CCS described here. Fisheries scientists must evaluate the relative environmental differences in each region, as they pertain to the climate signal and its variability, and compare them to a species' distribution and behavior as a function of life stage, to fully understand the consequences of climate change on populations.

CONCLUSION

State-space statistical models are applied to long environmental time series of monthly COADS northward wind stress and sea surface temperature (SST) from the California Current System (CCS) off the west coast of North America (22-48°N) for the period 1946-1990. The models estimate a non-parametric and non-linear trend, a non-stationary and non-deterministic seasonal signal, and an autoregressive (AR) term. The models are applied to long time series of SST from selected coastal sites as well, for comparison to the COADS series.

Based on a visual and statistical comparison of the model trend series, the CCS can be divided into three distinct geographical regions, which roughly correspond to the biological regions defined by Parrish *et al.* (1981) from mean meteorological and oceanic relationships and coastal fish reproduction patterns. The northern region (42-48°N) features a strong transition from strongly equatorward to poleward with distance north (compare 41°N, 43°N and 45°N stress time series in Fig. 4). The mean stress north of 44°N is poleward and has become increasingly poleward over time (Table 3). The transition zone in wind stress has expanded southward over time, strengthening the zonal gradient in poleward stress. The CCS north of 40°N features spatially uniform mean SST (Fig. 6), and SST trends show a series-length cooling tendency (Table 3). This region of uniform SST has expanded southward over time as well.

Winds trend series south of 40°N are equatorward and can be described in terms of a central and southern region (Fig. 4, Table 2). The central region (34-42°N) exhibits the strongest wind stress in the CCS. Equatorward stress has intensified over time more than in the northern and southern regions. This region features the greatest interannual to decadal variation as well. Like wind stress, interannual to decadal variability in SST is greatest in the central region (Fig. 6). Stress in the southern region (22-34°N) has become increasingly equatorward over time in a relatively monotonic pattern. Mean SST decreases consistently with increasing latitude in the central and southern regions. SST over about 30-38°N appears to warm rapidly in response to the 1957 and 1983 ENSO events as well as the 1976 regime shift. SSTs off Washington, Oregon and most of Baja California, on the other hand, take several months to years to warm by similar amounts.

While SST trends at all coastal sites display a significant warming tendency for the past several decades (Fig. 8), COADS (i.e., offshore) SST has warmed south of 36°N, but cooled north of 36°N (Fig. 6, Table 3). On shorter time scales, SST has decreased significantly since the 1983 ENSO north of about 34°N, but SST south of about 32°N has returned to near-1983 levels, after initially declining following this event. Prior to 1983, SST in the CCS warmed and cooled system-wide on decadal time scales, but has displayed a more incoherent pattern since 1983 (Fig. 7). A lack of correspondence between the COADS and coastal SST time series (Fig. 9) suggests there is considerable cross-shelf as well as latitudinal variability in the CCS. This is confirmed by the comparison of the 1° COADS SST data from two decades (Fig. 10).

SST trends are visually and statistically more correlated on interannual scales than are wind stress trends. Major ENSOs (i.e., 1957, 1983) and a well-documented regime shift in about 1976 dominate the SST trend series, particularly south of 38°N, but are not apparent in the wind trends. Instead ENSO wind variance is seen more clearly in the model AR and error series (Fig. 2), presumably because of the rapid atmospheric response to ENSO events. SST also shows decadal-scale periods of warm and cool anomalies that extend through the entire CCS. Wind stress anomalies are less extensive latitudinally and generally uncorrelated with SST (Table 3), suggesting that decadal-scale SST variability in the CCS is controlled by fluctuations in the basin- to global-scale pressure and wind fields, rather than local wind forcing.

In closing, we cannot consider the long-term trends described here without considering changes in the seasonal patterns at a location. Durand and Mendelsohn (this vol.) provide a discussion of how climate change can be interpreted in a number of ways. Schwing and Mendelsohn (this vol.) highlight an example of how seasonal changes over long time scales can have a clear signal that is independent of patterns in the long-term trends. The state-space model is a powerful tool for separating interannual-to-interdecadal fluctuations in environmental time series from seasonal patterns of variability. The results presented here demonstrate the importance of evaluating temporal and spatial variations over the entire spectrum, rather than simply at global climate scales, when examining long-term environmental fluctuations. This will improve our understanding of the linkages between shifts in atmospheric forcing and the coastal ocean's response on regional scales, and ultimately an improved assessment of the impact of climate change on living marine resources.

ACKNOWLEDGMENTS

We are extremely grateful to Philippe Cury and Claude Roy, who contributed greatly to this manuscript through their scientific discussions and collaborations, their assistance in preparing the data sets, and for their logistical support with the CEOS Workshop and the preparation and publication of this manuscript. We also thank Andrew Bakun for his critical review of the manuscript and his thoughtful scientific and technical comments. Tone Nichols assisted with preparation of the figures.

REFERENCES CITED

- Ainley D., B. DeLong, S. Herrick, L. Jacobson, E. Konno, J. Lanfersieck, M. Lowry, R. Parrish, C. Thomson, and P. Wolf. 1993. *Draft fishery description for the Pacific Coastal Pelagic Species Fishery Management Plan*. NMFS, SWFSC, Admin. Rep., LJ-93, 15.
- Bakun A. and C.S. Nelson. 1991. The seasonal cycle of wind-stress curl in subtropical eastern boundary current regions. *J. Phys. Oceanogr.*, 21: 1815-1834.
- Barnes J.T., L.D. Jacobson, A.D. MacCall and P. Wolf. 1992. Recent population trends and abundance estimates for sardine (*Sardinops sagax*). California. *Calif. Coop. Oceanic Fish. Invest. Rep.*, 33: 60-75.
- Baumgartner T.R., A. Soutar and V. Ferreira-Bartolina. 1992. Reconstruction of the history of Pacific sardine and northern anchovy populations over the past two millennia from sediments of the Santa Barbara Basin. California. *Calif. Coop. Oceanic Fish. Invest. Rep.*, 33: 24-40.
- Cardone V.J., J.G. Greenwood and M. Cane. 1990. On trends in the historical marine wind data. *J. Climate*, 3: 113-127.
- Ebbesmeyer C.C., D.R. Cayan, D.R. McLain, F.H. Nichols, D.H. Peterson and K.T. Redmond. 1991. 1976 step in the Pacific climate: Forty environmental changes between 1968-1975 and 1977-1984. In: J. Betancourt and V.L. Sharp (eds.). *Proc. 7th Ann. Pacific Climate Workshop, Calif. Dept. of Water Resources, Interagency Ecol. Stud. Prog. Tech. Rep.*, 26: 129-141.
- Hollowed A.B. and W.S. Wooster. 1992. Variability of winter ocean conditions and strong year classes of northeast Pacific fish stocks. *ICES Mar. Sci. Symp.*, 195: 433-444.
- Isemer H.-J. 1992. Comparison of estimated and measured marine surface wind speed. In: H.F. Diaz, K. Wolter and S.D. Wooldruff (eds.). *Proceedings of the International COADS Workshop*, Boulder, Colorado, 13-15 January 1992. U.S. Dep. Comm. 142-158.
- Kitagawa G. and W. Gersch. 1984. A smoothness priors - state space modeling of time series with trend and seasonality. *J. Am. Statist. Assoc.*, 79: 378-389.
- Kitagawa G. and W. Gersch. 1988. Smoothness priors in time series. In: J. Spall (ed.). *Bayesian analysis of time series and dynamic models*. Marcel Dekker, N.Y.
- Lenarz W.H., D. VenTresca, W.M. Graham, F.B. Schwing and F. Chavez. 1995. Explorations of El Niños and associated biological population dynamics off central California. *Calif. Coop. Oceanic Fish. Invest. Rep.*, 36: 106-119.
- MacCall A.D. 1979. Population estimates for the waning years of the Pacific sardine fishery. *Calif. Coop. Oceanic Fish. Invest. Rep.*, 20: 72-82.
- MacCall A.D. 1986. Changes in the biomass of the California Current ecosystems. In: K. Sherman and L.M. Alexander (eds.) *Variability and management of large marine ecosystems*. AAAS Selected Symposia 99, Westview Press, Boulder, CO: 33-54.
- MacCall A.D. and M.H. Prager. 1988. Historical changes in abundance of six fish species off southern California, based on CALCOFI egg and larva samples. *Calif. Coop. Oceanic Fish. Invest. Rep.*, 29: 91-101.
- McGowan J.A. 1985. El Niño 1983 in the southern California Bight. In: W.S. Wooster and D.L. Fluharty (eds.). *El Niño north: El Niño effects in the eastern subarctic Pacific Ocean*. University of Washington Press, Seattle, WA: 166-184.
- Mendelssohn R. and C. Roy. 1996. Comprehensive Ocean Data Extraction Users Guide. *U.S. Dep. Comm., NOAA Tech. Memo. NOAA-TM-NMFS-SWFSC-228*, La Jolla, CA, 67p.
- Miller A.J., D.R. Cayan, T.P. Barnett, N.E. Graham and J.M. Oberhuber. 1994. The 1976-77 climate shift of the Pacific Ocean. *Oceanography*, 7: 21-26.
- Parrish R.H., C.S. Nelson and A. Bakun. 1981. Transport mechanisms and reproductive success of fishes in the California Current. *Biol. Oceanogr.*, 1: 175-203.
- Pearcy W., J. Fisher, R. Brodeur and S. Johnson. 1985. Effects of the 1983 El Niño on coastal nekton off Oregon and Washington. In: W.S. Wooster and D.L. Fluharty (eds.). *El Niño north: El Niño effects in the eastern subarctic Pacific Ocean*. University of Washington Press, Seattle, WA: 188-204.
- Quinn W.H., V.T. Neal and S.E. Antunez de Mayolo. 1987. El Niño occurrences over the past four and a half centuries. *J. Geophys. Res.*, 92: 14449-14461.
- Radovich J. 1961. Relationships of some marine organisms of the northeast Pacific to water temperatures: particularly during 1957 through 1959. *Calif. Dep. Fish Game Fish. Bull.*, 112, 62 p.

- Roemmich D. and J. McGowan. 1995. Climatic warming and the decline of zooplankton in the California Current. *Science*, 267: 1324-1326.
- Royer T.C. 1993. High-latitude oceanic variability associated with the 18.6-year nodal tide. *J. Geophys. Res.*, 98: 4639-4644.
- Skillman J.B. 1993. *ENSO forced variations of the sea surface temperature and adjusted sea level along the west coast of the United States*. M.S. thesis, Naval Postgraduate School, Monterey, CA, 92 p.
- Slutz R.J., S.J. Lubker, J.D. Hiscox, S.D. Woodruff, R.L. Jenne, D.H. Joseph, P.M. Steurer and J.D. Elms. 1985. *Comprehensive Ocean-Atmosphere Data Set*; Release 1. NOAA Environmental Research Laboratories, Climate Research Program, Boulder, CO, 268 p.
- Trenberth K.E. 1990. Recent observed interdecadal climate changes in the northern hemisphere. *Bull. Amer. Meteor. Soc.*, 71: 938-993.
- Trenberth K.E. and J.W. Hurrell. 1994. Decadal atmospheric-ocean variations in the Pacific. *Clim. Dyn.*, 9: 303-319.
- Walker P.M., D.M. Newton and A.W. Mantyla. 1993. *Surface water temperatures, salinities and densities at shore stations, United States West Coast, 1992*. University of California, San Diego, Scripps Institution of Oceanography, La Jolla, CA, SIO Ref., 93 (18), 46 p.
- Woodruff S.D., R.J. Slutz, R.L. Jenne and P.M. Steurer. 1987. A Comprehensive Ocean-Atmosphere Data Set. *Bull. Amer. Meteor. Soc.*, 68: 1239-1250.
- Wu Z. and R.E. Newell. 1992. The wind problem in COADS and its influence on the water balance. *In*: H.F. Diaz, K. Wolter and S.D. Woodruff (eds.). *Proceedings of the International COADS Workshop*, Boulder, Colorado, 13-15 January 1992. U.S. Dep. Comm.: 189-200.